Microsc. Microanal. 18, 324–330, 2012
doi:10.1017/S1431927611012840

Microscopy AND Microanalysis

Bioconjugated and Cross-Linked Bionanostructures for Bifunctional Immunohistochemical Labeling

Rıdvan Say,[1,*] Gözde Aydoğan Kılıç,[2] Ayça Atılır Özcan,[1] Deniz Hür,[1,3] Filiz Yılmaz,[1] Adil Denizli,[4] and Arzu Ersöz[1]

[1]*Department of Chemistry, Anadolu University, Eskişehir, Turkey*
[2]*Department of Biology, Anadolu University, Eskişehir, Turkey*
[3]*Plant, Drug and Scientific Research Center, Anadolu University, Eskişehir, Turkey*
[4]*Department of Chemistry, Hacettepe University, Ankara, Turkey*

Abstract: The present study describes the development and use of a new bioconjugate combining targeted quantum dot labeling with an immunoperoxidase method and explores whether these bioconjugates could specifically and effectively label Cu/Zn superoxide dismutase (SOD1). The new bioconjugate is designed for the examination of samples both under fluorescent and bright-field microscopy at the same time. For this purpose chlorobis(2-2′-bipyridyl) methacryloyl tyrosine-ruthenium(II) and bis (2-2′-bipyridyl) methacryloyltyrosine-methacryloyltryptophan-ruthenium (II) photosensitive monomers and photosensitive poly(Bis (2-2′-bipyridyl)) methacryloyltyrosine-methacryloyltryptophan-ruthenium(II) were synthesized and characterized. The anti-SOD1 antibody and horseradish peroxidase (HRD) conjugated quantum dots were prepared by using this polymer. The anti-SOD1 antibody and HRD conjugated quantum dots were used in labeling and imaging of SOD1 in rat liver sections. Quantum dot particles were observed as a bright fluorescence in their specific binding locations inside the hepatocytes. The HRD-diaminobenzidine reaction product was observed as brown-colored particles at the same locations under bright-field microscopy. Structural details of the tissue sections could be examined at the same time. The conjugation protocol is simple; the bioconjugate is applicable for efficient cell labeling and can be adapted for imaging of other targets in different tissues. Also, the prepared nanobioconjugates have mechanic stability and can be used for a long period.

Key words: quantum dots, fluorescent labeling, immunoperoxidase method, SOD1, bioconjugate, optical imaging

Introduction

The development of multifunctional nanoparticles for the direct labeling of biomolecules is important for the future advances of biological and medical research (Defrus et al., 2007; Yoo et al., 2008; Stelter et al., 2010). Labeling using nanoparticles permits multiple labeling, with many fluorophores as well as with targeting proteins such as antibodies in various applications (Xing et al., 2007; Robertson et al., 2008). Several characteristics distinguish quantum dots (QDs) from commonly used fluorophores, such as broad absorption spectra, size- and composition-tunable, narrow fluorescence emission, and very high levels of brightness and photostability (Ornberg et al., 2004; Yu et al., 2007). Biological molecules, such as an antibody recognizing the target, can be linked to the surface of colloidal QDs to introduce specific functionalities (Parak et al., 2005; Diltemiz et al., 2008; Sweeney et al., 2008). Antibody conjugates of QDs exhibit modest but significant penetration into fixed and mildly permeablized cells and tissues (i.e., several microns) (Deerinck, 2008).

Immunoperoxidase methods have much in common with established immunofluorescence procedures. Both have the potential for specific demonstration of cell and tissue antigens (Taylor, 1978). Horseradish peroxidase (HRP) is a globular glycoprotein with a mass of 42 kDa, with four lysine residue for conjugation to a labeled molecule. It is often used in conjugates for molecular targeting. The use of HRP for enzyme mediated immunodetection, commonly referred to as immunoperoxidase labeling, is a well-established histochemical technique. During this reaction, diaminobenzidine (DAB) as an electron donor to the peroxidase-hydrogen peroxide complex undergoes oxidative polymerization and cyclization forming an intensely colored insoluble phenasine polymer (Grube, 1980). The DAB reaction product is discretely localized at HRP-labeled sites providing high-resolution images of subcellular antigen distribution and can be visualized directly by bright-field light microscopy.

Cu/Zn superoxide dismutase (SOD1) is an abundant protein that catalyzes the dismutation of superoxides to hydrogen peroxide. This enzyme is important to defend biological tissues against cell injuries mediated by oxygen-free radicals and has long been used as a biomarker of the oxidative status of cells (Chang et al., 1988). Liver has the highest concentration of such enzymes with the capacity to metabolize toxicants. In recent years, several groups have used QD probes for fluorescence immunostaining of tissue specimens (Xing et al., 2007). Although the localization of SOD1 has been demonstrated in our previous study and in

Received July 6, 2011; accepted November 23, 2011
*Corresponding author. E-mail: rsay@anadolu.edu.tr

different cells and tissues with various techniques, QDs have only recently been specialized to detect this enzyme in biological samples (Say et al., 2011).

From a different point of view, here we describe the development and use of bioconjugate, combining targeted QDs and the immunoperoxidase method for the labeling of SOD1 in rat liver. For this purpose, HRP-anti Cu/Zn SOD1-QD bioconjugate has been synthesized and SOD1 has been specifically labeled by using the bioconjugate in rat liver sections. The distribution of targeted QDs can be evaluated both under fluorescence and bright-field microscopy while examining histological structure of tissues. The study displays optimized experimental procedures for QD bioconjugation by the AmiNoAcid (monomer) Decorated and Light Underpining Conjugation Approach (ANADOLUCA) method and tissue preparation for the specimens. ANADOLUCA (Say, 2011) is a photosensitive, covalent, and cross-linking conjugation method to use in life sciences and biotechnology. The photosensitive, covalent, and cross-linking conjugation method is based on amino acid and ruthenium-chelate based monomers providing accurate antibody orientation and multiplexed conjugation. The method prevents denaturation during bonding and after bonding. Indeed, it provides efficiency of bounded proteins in many uses such as reusable enzymes, reusable separation solid phase systems based on affinity chromatography, theranostics, nanoprotein carrier, receptor targeted nanocargoes, manageable imaging, and detection technologies. The photosensitive amino acid monomer linkers can react chemically and are biocompatible to a lot of different micro- and nanosurface and to the protein when they act as a single-step cross-linking reaction using irradiation (Say et al., 2011).

Materials and Methods

Chemicals and Apparatus

SOD1 antibody was purchased from Santa Cruz Biotechnology, Inc. (Santa Cruz, CA, USA). Horseradish peroxidase (HRP), bovine serum albumin (BSA), Na_2HPO_4, NaH_2PO_4, $MgSO_4$, ammoniumpersulphate (APS), diaminobenzidine (DAB), 2,2′-azobisisobutyronitrile (AIBN), *N*-hydroxysuccinimide (NHS), and N-(3-dimethylaminopropyl)-N′-ethylcarbodiimide (EDC) were purchased from Aldrich (Milwaukee, WI, USA) and Sigma (St. Louis, MO, USA); paraformaldehyde and glutaraldehyde were bought from Merck (Whitehouse Station, NJ, USA); ethanol was bought from Fluka (St. Louis, MO, USA). London Resin (LR White) and gelatin embedding capsules were supplied from Electron Microscopy Sciences (Fort Washington, PA, USA).

Tissues were sectioned by using a Leica ultramicrotome and sections were observed under a Leica DM6000 B bright-field microscope.

Elemental analyses were performed by Vario ELIII. NMR spectra were recorded on a Bruker 500 MHz NMR spectrometer Ultrashield FT-NMR spectrometer (Bruker, Karlsruhe, Germany) at room temperature. All MALDI-TOF/MS mass spectra were acquired on an Applied Biosystems (Carlsbad, CA, USA) Voyager STR.

Chemical Synthesis of the Photosensitive Ruthenium Based Amino Acid Monomer

3-(4-hydroxyphenyl)-2-[(2-methylacryloyl)amino]propanoic acid (methacryloyl tyrosine, MATyr), N-[1-(1H-Indol-3-ylmethyl)-2-oxo-propyl]-2-methylacrylamide (methacryloyl tryptophan, MATrp) and 2-[(2-methylacryloyl)amino]-3-sulfanylpropanoic acid (methacryloyl cysteine, MACys) were prepared according to previously published method by our group (Hür et al., 2007).

Ruthenium chloride bipyridyl ($RuCl_2(bipyr)_2$) was synthesized according to the following procedure: 1 eq dichloro tetrakis (dimethylsulphoxide) ruthenium (II) ($RuCl_2(Me_2SO)_4$) and 2 eq 2-2′-bipyridyl were refluxed in chloroform (30 mL) for 1 h. The solvent was removed and the residue was dissolved in acetone. The orange complex was precipitated by adding ether. The precipitate was filtered off, washed with ether, and dried under vacuum (Evans et al., 1973).

For the synthesis of chlorobis(2-2′-bipyridyl) MATyr-ruthenium(II), 1 eq $RuCl_2(bipyr)_2$ was dissolved in methanol. The solution was cooled and ethylenetriamine was added. 1.2 eq MATyr in methanol solution was added dropwise into that solution and the mixture was refluxed at 55°C for 48 h. At the end of the reaction time, the solvent was removed under reduced pressure and the residue was dissolved in dichloromethane. The solution was washed three times with H_2O and dried with $MgSO_4$. After that, the solvent was evaporated and the product was washed with ether. It was dried under vacuum. M.p.: 125–128°C. The chemical reaction is shown in Figure 1.

Synthesis of Bis (2-2′-Bipyridyl) MATyr-MATrp-Ruthenium (II)

1 eq Chlorobis(2-2′-bipyridyl) MATyr-ruthenium(II) was dissolved in methanol. 1.2 eq MATrp solution in methanol was added into the above solution drop wise at room temperature. The mixture was refluxed at 80°C for 24 h. At the end of the reaction time, the solvent was removed under reduced pressure and the residue was dissolved in dichloromethane. The solution was washed with $3xH_2O$ and dried with $MgSO_4$. The solvent was evaporated; the product was washed with ether and dried under vacuum M. p.:110–112°C (Fig. 2).

Synthesis of the Photosensitive Poly(Bis (2-2′-Bipyridyl) MATyr-MATrp Ruthenium(II)) ($[Ru(bpy)_2MATrp\text{-}MATyr]_n$)

Bis (2-2′-bipyridyl)-MATrp-MATyr ruthenium(II) monomer was mixed in dimethyl sulfoxide to obtain a photosensitive oligomer (water dissolve). The polymerization reaction was carried out in the presence of AIBN as an initiator. For the MALDI-TOF-MS analysis, 2 μL of ($[Ru(bpy)_2MATrp\text{-}MATyr]_n$) solution was mixed with 23 μL of a 10 mg mL^{-1}

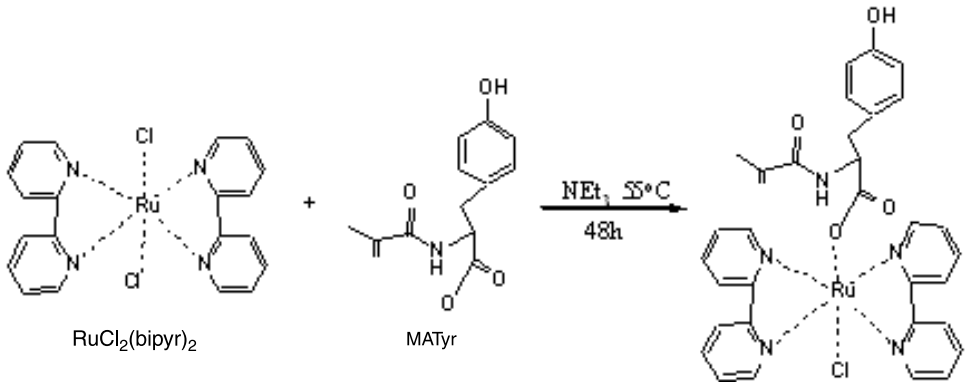

Figure 1. Synthesis of chlorobis(2-2′-bipyridyl) MATyr-ruthenium(II) photosensitive chelate.

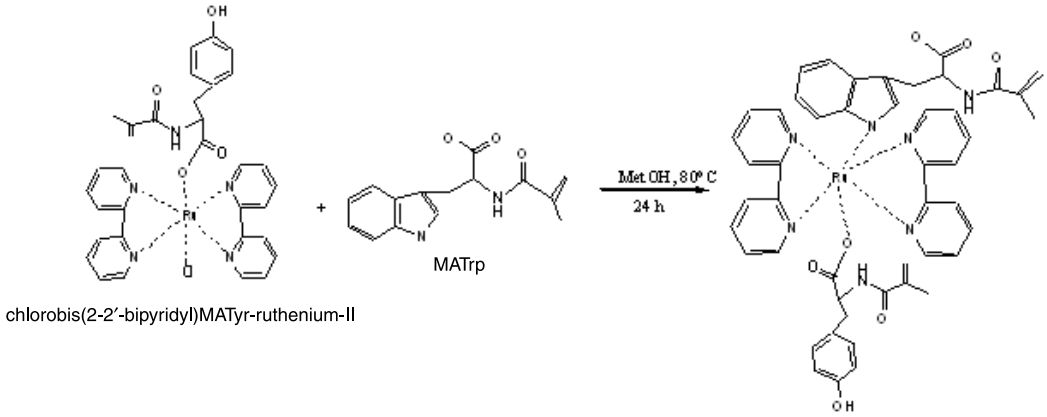

Figure 2. Synthesis of bis(2-2′-bipyridyl) MATyr-MATrp-ruthenium(II) photosensitive chelate.

solution of α-cyano-4-hydroxycinnamic acid (CHCA) in acetonitrile/0.3% TFA. The acceleration voltage was set to 20 kV, the delay time was 400 ns, grid voltage was 70%, laser intensity was 2.092, and at reflector mode.

Preparation of Anti-SOD1 Antibody and HRP Conjugated QDs

CdS QDs were synthesized according to a previously published method and activated with MACys and MATyr (Kulkarni et al., 2005; Diltemiz et al., 2008). Then, 100 μL of poly(Bis (2-2′-bipyridyl)-MATrp-MATyr ruthenium(II)) solution, 300 μL of 200 ppm anti-SOD antibody, and 100 μL of 100 ppm APS were added separately, into 2 mL of MACys and MATyr modified QD solution. The solution was mixed for 3 h. After that, 150 μL of 0.1 M NHS, 150 μL of 0.4 M EDC, and 150 μL of 5.000 ppm MATyr solutions were added into anti-SOD1 modified QD mixture and mixed for 3 h. Lastly, 200 ppm 150 μL of HRP solution in deionized water, 100 μL of poly(bis (2-2′-bipyridyl)-MATrp-MATyr ruthenium(II)), and 100 μL of 100 ppm APS were added into the modified QD solution and then mixed for 24 h.

Labeling of Tissue Sections

Animals

Adult male Wistar rats weighing between 200–225 g were acclimatized under laboratory conditions at least 3 days prior to use. They were anesthetized with ether, sacrificed, and the livers were dissected for immunohistochemical analyses.

Tissue Processing

1 mm^3 liver sections were fixed in 4% paraformaldehyde and 1% glutaraldehyde in PBS (pH 7.2) for 2 h at room temperature. The tissues were dehydrated two times in 50% ethanol for 30 min, two times in 70% ethanol for 30 min, and incubated in a 2:1 ratio of 70% ethanol:LR white for 1 h, and then were incubated in pure LR white overnight at room temperature. After that, they were embedded in gelatin capsules, fully filled and tightly capped. Polymerization was performed for 24 h in a 50°C incubator. The tissues were sectioned at 700 nm thickness using a glass knife.

Peroxidase-Fluorescence Labeling

For all incubations, the solutions were placed in small dishes and the sections were floated. They were washed three times with 1X PBS for 5 min each wash. The sections were then incubated in 1% BSA in PBS buffer at pH 7.2 for 1 h to block nonspecific protein binding sites and minimize nonspecific antibody binding. The sections were incubated with HRP and QD conjugated primary antibody in PBS for 2 h at room temperature and rinsed with PBS buffer three times for 1 min. They were incubated in DAB solution for 15 min, and 0.03% H_2O_2 was added to each well and mixed

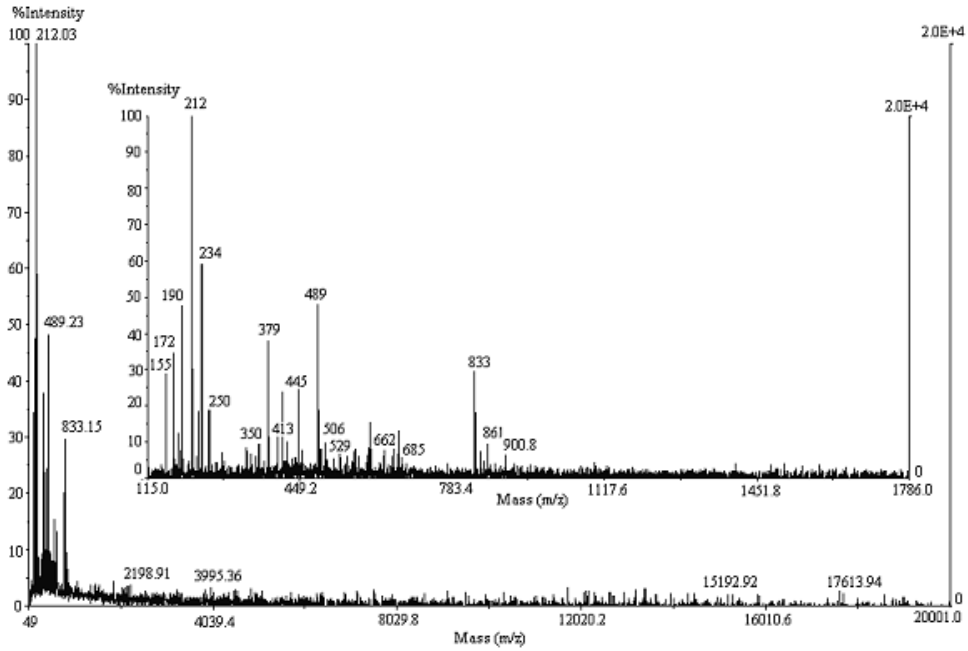

Figure 3. MALDI-TOF/MS spectrum of ($[Ru(bpy)_2MATrp\text{-}MATyr]_n$) polymer.

for 1 min. The sections were weakly stained with toluidine blue for light microscopic visualization and examined under a fluorescence microscope.

Results and Discussion

Characterization of Dichlorobis(2-2′-Bipyridyl) Ruthenium(II) ($RuCl_2(bipyr)_2$)

Analysis for $C_{20}H_{15}Cl_2N_4Ru$: found: C 48.20%, H 3.01%, N 12.89%, calculated: C 49.70%, H 3.13%, N 11.59%.

^{1}H NMR (500 MHz, $CDCl_3$), ppm:10.25 (d, 2H, J = 4.35 Hz), 9.93 (d, 2H, J = 4.29 Hz), 9.73 (d, 2H, J = 5.86 Hz), 9.65 (d, 2H, J = 4.52 Hz).

MALDI-TOF-MS: The ion peaks at 79, 128, and 156 m/e relating to bipyridyl. m/z 101 and 413 show Ru and $Ru(bpy)_2$, respectively. m/z 293, 327, 448, and 484 relating to RubpyCl, $RubpyCl_2$, $Ru(bpy)_2Cl$ and $Ru(bpy)_2Cl_2$, respectively. The MS-spectrum data confirm that the $Ru(bpy)_2Cl_2$ structure was produced exactly.

Characterization of Chlorobis(2-2′-Bipyridyl) MATyr-Ruthenium(II)

Analysis for $C_{34}H_{33}ClN_5O_4Ru$: found: C 56.75%, H 5.01%, N 10.23%, calculated: C 57.34%, H 4.67%, N 9.83%.

^{1}H NMR (500 MHz, $CDCl_3$), ppm: 9.7 (d, 4H, ^{3}J = 5.08 Hz), 8.56 (d, 4H, ^{3}J = 7.92 Hz), 7.92 (t, 4H, ^{3}J = 7.82 Hz), 7.3 (t, 1H, ^{3}J = 7.4 Hz), 7.23 (t, 2H, ^{3}J = 7.47 Hz), 7.18 (d, 2H, ^{3}J = 7.46 Hz), 7.12 (t, 4H, ^{3}J = 6.30 Hz), 5.3 (d, 1H, ^{2}J = 1.52 Hz), 5.3 (d, 1H, ^{2}J = 1.54 Hz), 1.8 (s, 3H).

MALDI-TOF-MS: The ion peaks at 79 m/e relating to bipyridyl. m/z 101, 413 and 448 data show Ru, $Ru(bpy)_2$, and $Ru(bpy)_2Cl$, respectively. m/z 250 and 351 peaks show MATyr monomer and Ru-MATyr, respectively.

Characterization of Bis (2-2′-Bipyridyl) MATyr-MATrp Ruthenium(II)

Analysis for $C_{49}H_{49}N_7O_7Ru$: found: C 61.56%, H 4.9%, N 11.67%, calculated: C 62.01%, H 5.2%, N 10.33%.

^{1}H NMR (500 MHz, $CDCl_3$), ppm: 9.4 (d, 2H, ^{3}J = 5.2 Hz), 8.52 (d, 2H, ^{3}J = 8.08 Hz), 8.1 (s, 4H), 7.98 (t, 4H, ^{3}J = 7.74 Hz), 7.62–7.01 (m, 11H), 5.71 (d, 1H, ^{2}J = 1.57 Hz), 5.43 (d, 1H, ^{2}J = 1.52 Hz), 4.7 (t, 1H, ^{3}J = 5.7 Hz), 1.9 (s, 6H).

MALDI-TOF-MS: The ion peaks at 250 and 272 relating to MAT and MATrp monomer; m/z 257 and 413 data show Ru-bpy and $Ru(bpy)_2$, respectively. m/z 351, 529, and 622 peaks show Ru-MATyr, Ru-bpy-MATrp, and Ru-MATyr-MATrp, respectively.

Characterization of Poly(Bis (2-2′-Bipyridyl) MATyr-MATrp-Ruthenium(II))

The polymer of Bis(2-2′-bipyridyl)-MATrp-MATyr ruthenium(II) has 19 monomer units. MALDI-TOF/MS spectrum of ($[Ru(bpy)_2MATrp\text{-}MATyr]_n$) polymer was given in Figure 3. The ion peaks at 250, 351, 506, 529, 662, and 685 m/z relating to MATyr monomer, Ru-MATyr, Ru-bpy-MATyr, Ru-bpy-MATrp, $Ru(bpy)_2MATyr$, $Ru(bpy)_2$ MATrp, respectively. m/z 155, 413, and 448 show bpy, $Ru(bpy)_2$ and $Ru(bpy)_2Cl$, respectively. m/z 172, 190, 212, and 379 relating to CHCA matrix.

Labeling of Tissue Sections

Targeting of QDs for the fluorescent labeling of biomolecules is crucial to investigate the mechanism of the proteins that are involved in the cell's biochemistry. However, the distribution of QDs in biological samples has been mainly examined by fluorescence imaging, which does not

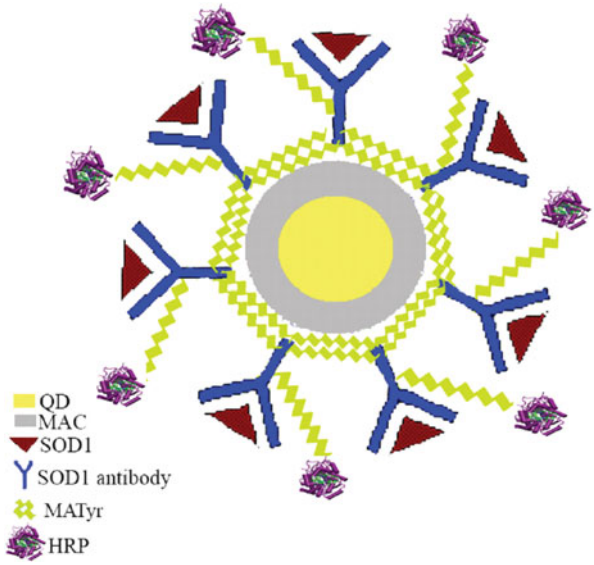

Figure 4. The schematic representation of HRP and SOD 1 antibody conjugated QDs.

account for optically degenerate QDs as a result of oxidative quenching (Parak et al., 2005; Chou et al., 2009; Stelter et al., 2010). Immunoperoxidase labeling is another commonly used immunohistochemical technique facilitating specific detection of the biomolecules and also allowing investigation of the histopathological situation of tissues.

The combination of optical imaging techniques provides more powerful tools for the sensitive and rapid visualization of biological molecules (Gilbert et al., 2001; Kruttwig et al., 2010). The present study investigates the synthesis and use of HRP and antibody conjugated QD nanoparticles in biological imaging by visualizing Cu-Zn SOD in liver tissue of rats. The schematic representation of HRP and antibody conjugated QDs are given in Figure 4. Combining targeted QDs and HRP enables the use of these superior fluorescent nanoparticles and immunoperoxidase techniques together in one step, allowing examination of labeled tissues both under light and fluorescent microscopy and evaluation of labeling efficacy.

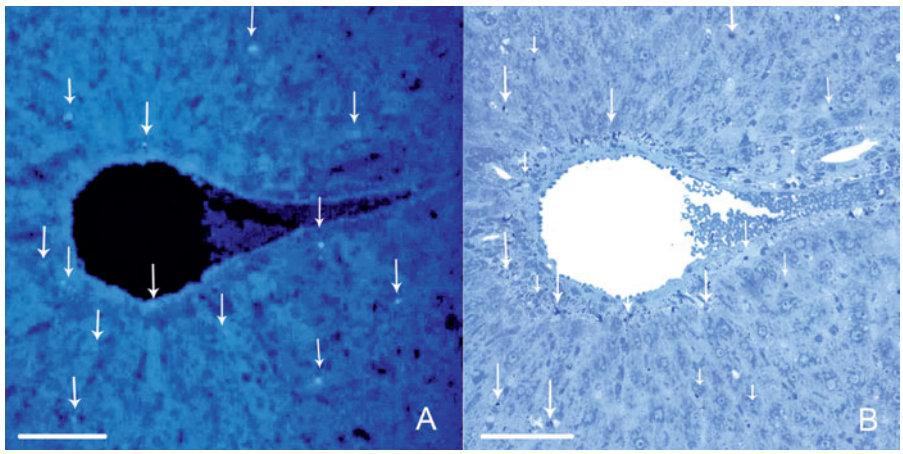

Figure 5. A: Fluorescence image of the tissue stained with HRP and anti-Cu-Zn-SOD conjugated quantum dots. Bright blue dots of specific binding sites inside the hepatocytes (arrowhead). Filter cube I3 (BP 450–490 nm, Dichromatic mirror 510 nm, LP 515 nm) was used to detect QD. Scale bar = 100 μm. **B:** Brown particles of HRP-DAB reaction product in specific binding sites (arrowhead). Scale bar: 100 μm.

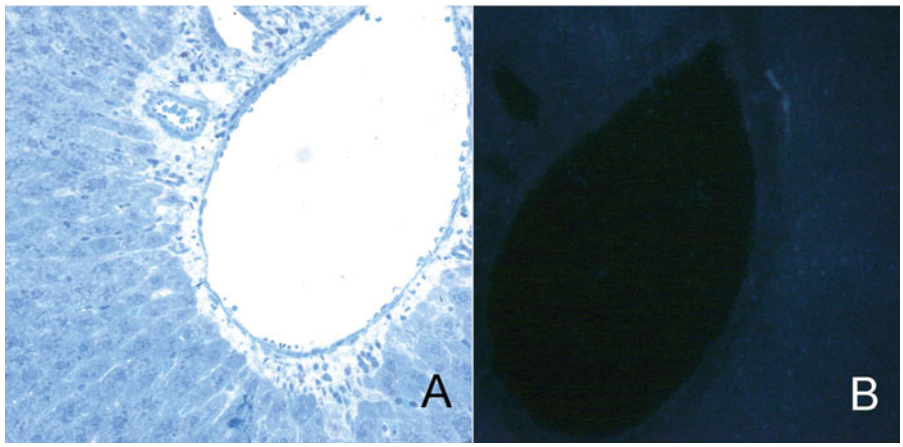

Figure 6. A: Light microscopy image of control group hepatocytes without any specific bindings. Scale bar = 100 μm. **B:** Control group tissue under fluorescence microscopy. Scale bar = 100 μm.

QD particles were observed as a bright fluorescence in their specific binding locations inside the hepatocytes (Fig. 5A). There were some larger bright dots of nonspecific binding sites. Cytoplasm of the cells contained many bright blue dots due to high content of the enzyme. Some nonspecific bindings were seen as bigger bright aggregates. Nuclei were seen darker because of their smaller content of Cu-Zn SOD and lower penetration ability of QDs to the cell nuclei (Xu et al., 2008). When tissues were incubated with unconjugated QDs as a control, no detectable signals were observed in hepatocytes except very weak dark blue background fluorescence (Fig. 6B).

When the subcellular distribution of SOD1 activity was first explored by fractionation of the liver, the cytosol was found to contain Cu/Zn-SOD (Okado-Matsumoto & Fridovich, 2001). Further studies with immunohistochemical techniques also demonstrated that rat liver SOD1 is localized predominantly in the cytosol, and it is also found in other compartments of the cell such as the nucleus, endoplasmic reticulum, mitochondria, and lysosomes in smaller amounts (Kawamata & Manfredi, 2008). These studies also support our results related to distribution of SOD1.

The HRP-DAB reaction product was observed as brown-colored particles on specific binding sites inside the hepatocytes (Fig. 5B). Brown particles were not observed in light microscopy images of the control group without any antibody binding (Fig. 6A). Usual structural details of the liver could also have been examined in toluidine blue stained bright-field microscopy sections.

Fluorescence labeling is one of the most common techniques used in cell biology (Parak et al., 2005; Yoo et al., 2008). However, conventional organic fluorophores suffer from significant limitations. These molecules are susceptible to photobleaching that limits the time for detection and interferes with repeated measurements. Broad emission and narrow absorption obstruct the use of organic fluorophores in multicolor applications. Quantum yield of organic fluorophores is usually less than 15% in aqueous environments. There is usually one ligand per fluorophore, so detectability is a strong function of target concentration (Frangioni, 2003; Wang et al., 2004; Diltemiz et al., 2008). QDs on the other hand have narrow emission and broad absorption spectra, excellent photostability, and high luminesence properties (Wang et al., 2004). Thus, targeting of QDs for the fluorescence labeling of biomolecules is crucial in order to investigate the mechanism of the proteins that are involved in the cell's biochemistry. The distribution of QDs in biological samples has been mainly examined by fluorescence imaging, which does not account for optically degenerate QDs as a result of oxidative quenching (Parak et al., 2005; Chou et al., 2009; Stelter et al., 2010). Immunoperoxidase labeling is another commonly used immunohistochemical technique facilitating specific detection of the biomolecules and also allowing investigating the histopathological situation of tissues.

The present study is an application of ANADOLUCA method, and in this method ruthenium based materials have been used either for the cross-linking or bioconjugation of HRP and other proteins due to their electron transferring property. By this way, it is aimed to obtain reusable, stabilized, and long-lasting materials. The other main advantage of this method (ANADOLUCA) is that nanobioconjugates can be prepared at mild conditions such as in daylight, independent of pH and temperature, without affecting conformation and function of the protein.

The combination of optical imaging techniques provides more powerful tools for the sensitive and rapid visualization of biological molecules (Gilbert et al., 2001; Kruttwig et al., 2010). Combining targeted QDs and HRP enables the use of these superior fluorescence nanoparticles and the immunoperoxidase technique together in one step, allowing examination of labeled tissues both under light and fluorescence microscopy and evaluation of labeling efficacy.

Conclusion

Our presented method, "two directional peroxidase-fluorescent labeling," enables visualization of fluorescence signals of the biomolecules, while providing light microscopy labels and histological details at the same time. Two-dimensional imaging using single protocol allows us to compare both light and fluorescence microscopy details while saving time. This method will be a useful tool for the imaging of SOD1 in tissue sections, providing fluorescence signaling, light microscopy labeling efficacy, and histological details and can be adapted to detect other targets in different tissues. The other main advantage of this method, the nanobioconjugates, can be prepared at mild conditions (for example, in daylight), independent of pH and temperature, without affecting conformation and function of the protein. Also, the prepared nanobioconjugates have mechanic stability and can be used for a long period.

References

Chang, L.Y., Slot, W.J., Geuze, H.J. & Crapo, J.D. (1988). Molecular immunocytochemistry of the CuZn superoxide dismutase in rat hepatocytes. *J Cell Biol* **107**(6), 2169–2179.

Chou, L.Y.T., Fischer, H.C., Perrault, S.D. & Chan, W.C.W. (2009). Visualizing quantum dots in biological samples using silver staining. *Anal Chem* **81**, 4560–4565.

Deerinck, T.J. (2008). The application of fluorescent quantum dots to confocal, multiphoton, and electron microscopic imaging. *Toxicol Pathol* **36**, 112–116.

Defrus, A.M., Chen, A.A., Min, D.H., Ruoslahti, E. & Bhaita, S.N. (2007). Targeted quantum dot conjugates for siRNA Delivery. *Bioconjugate Chem* **18**, 1391–1396.

Diltemiz, S.E., Say, R., Büyüktiryaki, S., Hür, D., Denizli, A. & Ersöz, A. (2008). Quantum dot nanocrystals having guanosine-imprinted nanoshell for DNA recognition. *Talanta* **75**, 890–896.

Evans, I.P., Spencer, A. & Wilkinson, G. (1973). Dichlorotetrakis (dimethyl sulphoxide) ruthenium (II) and its use as a source material for some new ruthenium (II) complexes. *J Chem Soc Dalton Trans* 204–209.

Frangioni, J.V. (2003). *In vivo* near-infrared fluorescence imaging. *Curr Opin Chem Biol* **7**, 626–634.

Gilbert, E.S., Khlebnikov, A., Cowan, S.E. & Keasling, J.D. (2001). Analysis of biofilm structure and gene expression using fluorescence dual labeling. *Biotechnol Prog* **17**, 1180–1182.

Grube, D. (1980). Immunoperoxidase methods: Increased efficiency using fluorescence microscopy for 3,3-diaminobenzidine (DAB) stained semithin sections. *Histochemistry* **70**, 19–22.

Hür, D., Ekti, S.F. & Say, R. (2007). N-Acylbenzotriazole mediated synthesis of some methacrylamido amino acids. *Lett Org Chem* **4**(8), 585–587.

Kawamata, H. & Manfredi, G. (2008). Different regulation of wild-type and mutant Cu,Zn superoxide dismutase localization in mammalian mitochondria. *Hum Mol Gen* **17**(21), 3303–3317.

Kruttwig, K., Bruggemann, C., Kaijzel, E., Vorhagen, S., Hilger, T., Löwik, C. & Hoehn, M. (2010). Development of a three-dimensional *in vitro* model for longitudinal observation of cell behavior: Monitoring by magnetic resonance imaging and optical imaging. *Mol Imaging Biol* **12**, 367–376.

Kulkarni, S.K., Ethiraj, A.S., Kharrazi, S., Deobagkar, D.N. & Deobagkar, D.D. (2005). Synthesis and spectral properties of DNA capped CdS nanoparticles in aqueous and non-aqueous media. *Biosens Bioelect* **21**, 95–102.

Okado-Matsumoto, A. & Fridovich, I. (2001). Subcellular distribution of superoxide dismutases in rat liver: Cu,Zn-SOD in mitochondria. *J Biol Chem* **276**(42), 38388–38393.

Ornberg, R.L., Wu, X. & Bruchez, M.P. (2004). Qdot conjugates: A novel fluorescence detection technology for biological imaging. *Microsc Microanal* **10**, 1272–1273.

Parak, W.J., Pellegrino, T. & Plank, C. (2005). Labelling of cells with quantum dots. *Nanotechnology* **16**, R9–R25.

Robertson, D., Savage, K., Reis-Filho, J.S. & Isacke, C.M. (2008). Multiple immunofluorescence labelling of formalin-fixed paraffin-embedded (FFPE) tissue. *BMC Cell Biol* **9**, 13–22.

Say, R. (2011). Photosensitive amino acid-monomer linkage and bioconjugation applications in life sciences and biotechnology. *World Intellectual Property Organization–PatentScope*, www.wipo.int/patentscope/search/en/WO2011070402 (Pub. No.: WO/2011/070402; Int. Appl. No.: PCT/IB2009.055707).

Say, R., Aydoğan Kiliç, G., Atilir Özcan, A., Hür, D., Yilmaz, F., Kutlu, M., Yazar, S., Denizli, A., Emir Diltemiz, S. & Ersöz, A. (2011). Investigation of photosensitively bioconjugated targeted quantum dots for the labeling of Cu/Zn superoxide dismutase in fixed cells and tissue sections. *Histochem Cell Biol* **135**(5), 523–530.

Stelter, L., Pinkernelle, J.G., Michel, R., Schwartlander, R., Raschzok, N., Morgul, M.H., Koch, M., Denecke, T., Ruf, J., Baumler, H., Jordan, A., Hamm, B., Sauer, I.M. & Teichgraber, U. (2010). Modification of aminosilanized superparamagnetic nanoparticles: Feasibility of multimodal detection using 3T MRI, Small animal PET, and fluorescence imaging. *Mol Imaging Biol* **12**, 25–34.

Sweeney, E., Ward, T.H., Gray, N., Womack, C., Jayson, G., Hughes, A., Dive, C. & Byers, R. (2008). Quantitative multiplexed quantum dot immunohistochemistry. *Biochem Biophys Res Commun* **374**, 181–186.

Taylor, C.R. (1978). Immunoperoxidase techniques practical and theorical aspects. *Arch Pathol Lab Med* **102**(3), 113–121.

Wang, H.Z., Wang, H.Y., Liang, R.Q. & Ruan, K.C. (2004). Detection of tumor marker CA125 in ovarian carcinoma using quantum dots. *Acta Biochim Biophys Sin* **36**(10), 681–686.

Xing, Y., Chaudry, Q., Shen, C., Kong, K.Y., Zhau, H.E., Chung, L.W., Petros, J.A., O'Regan, R.M., Yezhelyev, M.V., Simons, J.W., Wang, M.D. & Nie, S. (2007). Bioconjugated quantum dots for multiplexed and quantitative immunohistochemistry. *Nat Prot* **2**(5), 1152–1165.

Xu, Y., Wang, Q., He, P., Dong, Q., Liu, F., Liu, Y., Lin, L., Yan, H. & Zhao, X. (2008). Cell nucleus penetration by quantum dots induced by nuclear staining organic fluorophore and UV-irradiation. *Adv Mater* **20**, 3468–3473.

Yoo, J., Kambara, T., Gonda, K. & Higuchi, H. (2008). Intracellular imaging of targeted proteins labeled with quantum dots. *Exp Cell Res* **314**, 3563–3569.

Yu, X., Chen, L., Deng, Y., Li, K., Wang, Q., Li, Y., Xiao, S., Zhou, L., Luo, X., Liu, J. & Pang, D. (2007). Fluorescence analysis with quantum dot probes for hepatoma under one- and two-photon excitation. *J Fluoresc* **17**, 243–247.